NANO LETTERS

2008
Vol. 8, No. 3
941-944

Interaction of Nanoparticles with Lipid Membrane

Yuri Roiter,[†] Maryna Ornatska,[†] Aravind R. Rammohan,[‡] Jitendra Balakrishnan,[‡] David R. Heine,[‡] and Sergiy Minko*,[†]

Department of Chemistry and Biomolecular Science, Clarkson University, Potsdam, New York 13699-5810, Corning Inc., Corning, New York 14831

Received January 10, 2008; Revised Manuscript Received January 22, 2008

ABSTRACT

A nanoscale range of surface feature curvatures where lipid membranes lose integrity and form pores has been found experimentally. The pores were experimentally observed in the L-α-dimyristoyl phosphatidylcholine membrane around 1.2−22 nm polar nanoparticles deposited on mica surface. Lipid bilayer envelops or closely follows surface features with the curvatures outside of that region. This finding provides essential information for the understanding of nanoparticle−lipid membrane interaction, cytotoxicity, preparation of biomolecular templates and supported lipid membranes on rough and patterned surfaces.

Spontaneous fusion of lipid vesicles on glass, silica, and similar polar surfaces has been the subject of extensive research.[1] It is evident that supported lipid bilayers (SLB) retain many of the characteristics of natural cell membranes such as lateral fluidity, incorporation of proteins, phase separation, and impermeability to ionic species.[2–4] The number of applications of lipid membranes supported on planar and spherical substrates has grown significantly in recent years and includes important analytical assays and delivery systems.[5–7] However, the instability and often poorly defined morphology of supported lipid bilayers limit their clinical, environmental, and bioanalytical applications. To date, most of the research focuses on optimization of lipid composition and chemical modification of the substrate, whereas very little attention is paid to the effects and optimization of surface topography. Perhaps even more critical is the current concern about the potential cytotoxicity of nanomaterials[8] given their expanding role in modern industry and households. For these reasons, the study of "pore" or "hole" formation in lipid bilayers caused by nanoparticles and the search for both critical particle sizes and morphology are of special significance.

Because of the complex nature and uncertainty in the structure of lipid bilayers,[9–11] any computational modeling is limited to small fragments of a lipid membrane.[12–14] The formation of pores in lipid membranes under different conditions has been described in the number of simulation studies.[15–17] Experimental research has been limited mostly to micrometer-size glass beads where the mechanism of SLB formation was similar to that known for planar substrates. Until recently, very little experimental data could be found concerning the membrane behavior on highly curved surfaces. However, in 2005, it was found that 100 nm silica particles are enveloped by lipid bilayers.[18] More recent reports have shown the formation of a lipid bilayer on polysilicon nanowires over 50 nm in diameter[19] and the formation of SLB pores by polar dendrimers and other polymer molecules spread on a substrate surface.[20]

Our study focuses on the interaction of lipid bilayers prepared from L-α-dimyristoyl phosphatidylcholine (DMPC) with nanostructured silica surfaces using AFM, a powerful tool for in situ study of tiny morphological details of soft matter on a single molecule level.[21,22] AFM was successfully used to monitor in situ the formation of SLB in the lipid's liquid-gel state (28 °C).[23,24] For our purposes, nanostructured surfaces were prepared by decorating polished silicon wafers with silica nanoparticles ranging from 1 to 140 nm in diameter (see Materials and Methods in Supporting Information). A series of AFM images were then taken from nearly the same location, starting with the sample in the initial stage without lipid and finishing with the surface covered by lipid bilayer. After the bilayer had reached its final stage of formation, its quantity and location did not change further with additional time and increase of lipid concentration. Successive AFM 3D data matrices were aligned precisely by matching surface features and then subtracted to reveal the location of formed bilayer using software that we developed for this purpose (see Supporting Information).

Our results are grouped based on nanoparticle size-to-lipid bilayer thickness ratios, where we applied different experi-

* To whom correspondence should be addressed. E-mail: sminko@clarkson.edu.
[†] Department of Chemistry and Biomolecular Science, Clarkson University.
[‡] Corning Inc.

10.1021/nl080080l CCC: $40.75
Published on Web 02/07/2008

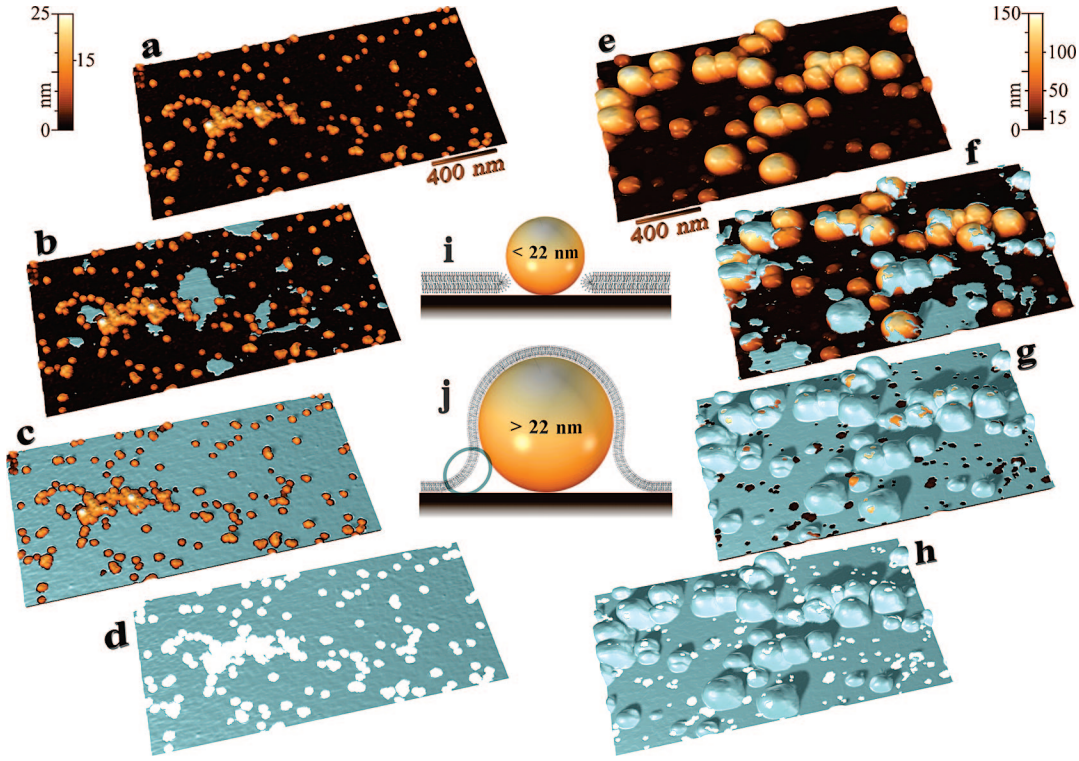

Figure 1. Lipid bilayer formation in the presence of particles larger than lipid bilayer thickness. AFM images (left) of lipid bilayer formation over a surface with 5–20 nm silica nanoparticles (a−d): (a) substrate with particles and no lipid, (b) surface partially covered by lipid bilayer (shown in silver color), (c) lipid bilayer formed on the substrate, (d) image of the lipid bilayer after "subtraction" of the particles and the substrate. AFM images (right) of lipid bilayer formation over the surface with mixed 5–140 nm silica particles (e−h): (e) the substrate with particles and no lipid, (f) partial coverage of the surface by lipid bilayer, (g) lipid bilayer formed on the substrate, and (h) image of the lipid bilayer after "subtraction" of the particles and the substrate. Schematics in the center illustrate how the lipid bilayer forms a pore around particles smaller than 22 nm (i) and how it may envelope the larger particles (j). The structure of bilayer area encircled in (j) is speculative because it cannot be resolved or assumed from AFM experiments.

ments to resolve the structure of SLB. First, we consider SLB formation on substrates decorated with nanoparticles of diameters *larger* than the lipid bilayer thickness (~5 nm, including the interfacial layer of water). Two series of AFM images (Figure 1) depict typical sequences of lipid membrane progression on a silica surface with 5–20 nm nanoparticles (Figure 1a−d) and 5–140 nm nanoparticles (Figure 1e−h). An adapted 3D presentation of the AFM images is being used in figures here, while the original AFM images can be found in Supporting Information.

The addition of a moderate quantity of lipid into the medium over the initial sample (Figure 1a) leads to the formation of lipid bilayer islands (Figure 1b). Nearly all nanoparticles remain uncoated with lipids, both at partial and final (Figure 1c) sample coverage. A detailed 3D view of the lipid membrane "extracted" from the substrate is shown in Figure 1d. Indeed, one sees that the bilayer has covered a relatively flat surface and has developed multiple pores around the nanoparticles. This finding led to the next step of investigation: the search for the critical size of larger particles that are covered by the lipid membrane (Figure 1e−h).

Unlike the previous case, even the early stages of SLB formation on a substrate with 5–140 nm nanoparticles (Figure 1e) show partial coverage on the larger particles (Figure 1f). The final bilayer covers larger particles nearly completely, whereas holes remained only around smaller nanoparticles (Figure 1g). This is clearly seen in the 3D image of the lipid bilayer (Figure 1h). Analysis of the recorded image allows us to determine the critical diameter to be about 22 nm (see Supporting Information, Figure S5). Larger particles are mostly covered with lipid bilayers (Figure 1j), while smaller particles mainly "pierce" it (Figure 1i). In some instances, larger particles cannot be covered completely (Figure 1g,h). Using transmission electron microscopy (TEM) and confocal microscopy (CM), it was discovered that pores in bilayers on larger particles are caused by high-curvature surface features, resembling 1–10 nm nanoparticles, which should pierce the lipid bilayer. However, 200 nm nanoparticles having smooth surfaces exhibited better integrity of the lipid bilayer found by CM (see Supporting Information Figure S12). The presence of a continuous bilayer at the edges of larger particles, where AFM does not resolve the topography (Figure 1j), was assumed.

Curvature of the lipid membrane is described in the literature as a balance of forces arising from adhesion energy and elastic deformation of the membrane. Corresponding simulation studies of colloidal particle interaction with a lipid membrane has revealed wrapping of the particles.[25] Further theoretical analyses yielded a structural phase diagram demarking the regions of fully enveloped, partially wrapped, or free colloids.[26,27] The evaluation of the transition state

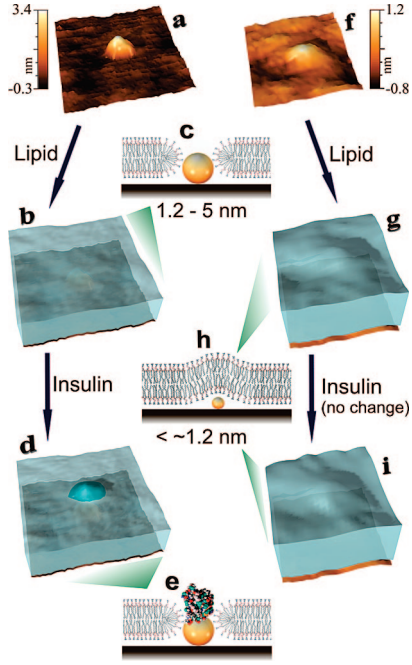

Figure 2. Lipid bilayer formation in the presence of particles smaller than lipid bilayer thickness. (a) AFM image of the sample in the initial stage (no lipid) with 3.4 nm particle, (b) lipid bilayer formed on the substrate with 3.4 nm particle with corresponding schematics in (c), (d) AFM topography after adsorption of an insulin molecule onto the particle through the hole in SLB (schematic is in (e)), (f) AFM image of the substrate with 1.2 nm particle (no lipid), (g) topography of the formed lipid bilayer over 1.2 nm particle (schematics is in (h)), and (i) image after the injection of insulin (no changes in topography).

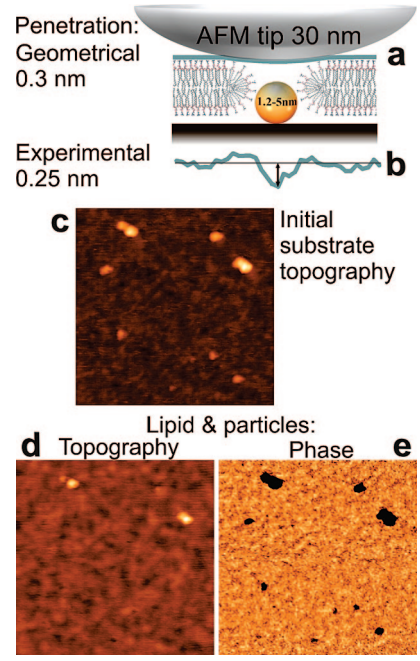

Figure 3. AFM data confirming the formation of pores around 1.2–5 nm nanoparticles: (a) theoretical and (b) experimental AFM topography of the pore in membrane, (c) topography image of the substrate with particles (no lipid), (d) topography and (e) phase imaging of the lipid deposited on the sample with 1–8 nm nanoparticles (scan size 475 × 475 nm^2).

between the envelopment and the free state of particles gave the critical diameter, $d_0 \approx 3\lambda$, where λ is a specific length of the membrane defined by the bending modulus and adhesion constant.[28] For a typical lipid membrane, $\lambda \approx 10$ nm, hence $d_0 \approx 30$ nm. Through use of AFM, we were able to identify the critical particle diameter for this transition being ~22 nm for particles on surface. However, the theory considers a continuous bilayer with no pores. An alternative theory suggests the formation of pores around strongly charged particles of ~2–8 nm.[16] It considers that those particles are enveloped by lipid bilayer during the pore formation. Results presented here demonstrate that a lipid bilayer forms pores around small polar particles but does not wrap them. This finding is valid not only for DMPC but also for the polar lipid extract from bovine liver at 37 °C (see Supporting Information Figure S11). The found behavior of the lipid membrane provides new possibilities for the creation of variously patterned and modified biological and medical planar and colloidal substrates.

Now we turn to SLB formation on nanoparticles of diameters smaller than the lipid bilayer. Figure 2a represents an AFM image of a single 3.4 nm particle. After the addition of DMPC, AFM shows that the lipid bilayer "covers" the nanoparticle (Figure 2b) with no signs of elevation but rather with a small decrease of its thickness over the particle. This result suggests that the bilayer does not follow the particle on the surface. The presence of hydrophilic particles in the continuous lipid bilayer is thermodynamically unfavorable because the bilayer is hydrophobic inside. The most probable structure in SLB is a pore around the particle. In the presented experiment, we used an AFM tip of ~30 nm curvature radius, which theoretically could penetrate only 0.3 nm into the pore around a 3 nm particle (Figure 3a). Such penetration can be distorted by the instrumental noise in one scan line. However, an average of eight experimental profiles over particles smaller than 5 nm (see Supporting Information Figures S6−S8) provided a tip penetration of 0.25 nm (Figure 3b), which is very close to the theoretical value of 0.3 nm and thus confirming the presence of pores. Phase imaging provides differentiation between materials (silica and SLB) due to their different interaction with the AFM tip. A pronounced contrast in the phase image (dark spots in Figure 3e, phase) correlates exactly with the locations of silica particles in the initial (before lipid deposition) topographical images (white spots in Figure 3c). The bigger particles (two big white spots and two big dark spots in the topographical images and phase image shown in Figure 3d,e, respectively), which pierce the membrane, can be used for alignment of the images. For smaller particles (seen as white spots in initial topography and not seen in the topographical image after lipid deposition), the dark spots suggest the formation of holes in the membrane (Figure 2c). This hypothesis was confirmed with protein probes introduced in the AFM liquid cell. Insulin readily sticks to the silica surface. However, this protein does not adsorb on the SLB. Figure 2d represents an AFM image of an insulin molecule adsorbed exactly over the 3.4 nm particle, thus "elevating" its height ~2 nm above the lipid level. Insulin, which is a ~3.5 nm globular protein, allowed the pinpointing of "holes"

in the lipid bilayer around small particles (see Supporting Information Figure S10). This protein diffused into the pores and adsorbed on the silica particles. Figure 2e shows the schematics of the insulin model imbedded in a pore. This behavior was also confirmed using a confocal microscopy with fluorescently labeled insulin (see Supporting Information Figure S13).

Analysis of the substrate with particles under ~1.2 nm in diameter (Figure 2f) shows that the lipid membrane follows the topographical features of the underlying substrate at this scale (Figure 2g). In other words, the topography of the membrane repeats the topography of the silicon substrate (Figure 2h). Injection of insulin probes in this case does not lead to any meaningful changes in topography (Figure 2i). This behavior of the membrane was confirmed by dynamic simulations of a continuum SLB on silica substrates in an implicit solvent (see Supporting Information Discussion). The computational results predict that the bilayer conforms to the substrate topography for feature sizes <3 nm, which is slightly larger than that observed through our experiments. This discrepancy may be due to the difference in formulation of the model membrane when compared to the adsorbed bilayers described above. The model suggests that the inability to conform to larger surface curvatures is due to the unfavorable bending energy of the membrane compared to the attractive force pulling the membrane to the surface. In the case of the model, the results show considerable deviations of the membrane from the substrate. In the experimental study described above, the bilayers lack mechanisms to sustain their lateral integrity (e.g., transmembrane proteins, sugars, collagen, etc.). The adverse bending energy needed to coat large features would thus result in local pore formation.

Our results indicate that due to the barrier function of the studied lipid bilayer particles with radii in the range between 1.2 and 22 nm were not covered by the bilayer membrane, while particles with radii outside that range were. Our results have shown that the structure of a lipid bilayer prepared from a natural mixture of lipids (bovine liver polar extract at 37 °C, see Supporting Information Discussion and Figure S11) is similar to that observed for DMPC. It is yet to be determined specifically whether this will a have direct impact on our understanding of nanoparticle cytotoxicity after the detailed studies of the particle interaction with cell membranes.[4,10,29] At any rate, obtained results can already find wide application in the rapidly developing bioanalytical field. Such a technique can be used for more effective manipulation of single proteins on the surfaces, thus opening new possibilities of targeting single protein molecules on specific nanoscale topography and targeting microarrays. The results will aid better understanding of the activity of biological membranes where the enzymes activity is regulated by membrane curvature.[30] At industrial scales, one can achieve much higher efficiency of SLB systems just by the control of surface roughness and composition of plane substrates and colloidal particles. This study may catalyze the development of new methods, allowing for precise control over the surface density of proteins with discrete spatial placing of the molecules. We anticipate that, by manipulating nanoscale roughness, a substrate with multiple nonspecific binding sites can be created and easily converted into specific binding sites using conventional methods.

Acknowledgment. This work was supported by Corning Inc. and NY Center for Advanced Materials Processing at Clarkson University. We thank Dr. Sokolov and Mr. Bill Plunkett (Clarkson University) for help with fluorescent confocal microscopy and TEM analysis. We thank Dr. Akhremitchev (Duke University) for help with design of custom-built temperature stage for AFM studies.

Supporting Information Available: Description of materials and techniques; raw, minimum, and specially processed experimental images; AFM experiment with polar lipid extract from bovine liver; computational model of bilayer behavior on surface. This material is available free of charge via the Internet at http://pubs.acs.org.

References

(1) Bayerl, T. M. *Nature* **2004**, *427*, 105–106.
(2) Israelachvili, J. *Q. Rev. Biophys.* **2005**, *38*, 331–337.
(3) Schonherr, H.; Johnson, J. M.; Lenz, P.; Frank, C. W.; Boxer, S. G. *Langmuir* **2004**, *20*, 11600–11606.
(4) Hamai, C.; Yang, T. L.; Kataoka, S.; Cremer, P. S.; Musser, S. M. *Biophys. J.* **2006**, *90*, 1241–1248.
(5) Groves, J. T.; Dustin, M. L. *J. Immunol. Methods* **2003**, *278*, 19–32.
(6) Sackmann, E. *Science* **1996**, *271*, 43–48.
(7) Boxer, S. G. *Curr. Opin. Chem. Biol.* **2000**, *4*, 704–709.
(8) Brunner, T. J.; Wick, P.; Manser, P.; Spohn, P.; Grass, R. N.; Limbach, L. K.; Bruinink, A.; Stark, W. J. *Environ. Sci. Technol.* **2006**, *40*, 4374–4381.
(9) Israelachvili, J. N.; Mitchell, D. J.; Ninham, B. W. *J. Chem. Soc., Faraday Trans. 2* **1976**, *72*, 1525–1568.
(10) Seifert, U. *Adv. Phys.* **1997**, *46*, 13–137.
(11) Nagle, J. F.; Tristram-Nagle, S. *Biochim. Biophys. Acta: Biomembr.* **2000**, *1469*, 159–195.
(12) Reynwar, B. J.; Illya, G.; Harmandaris, V. A.; Muller, M. M.; Kremer, K.; Deserno, M. *Nature* **2007**, *447*, 461–464.
(13) Swain, P. S.; Andelman, D. *Phys. Rev. E* **2001**, *63*, 051911.
(14) Tieleman, D. P.; Marrink, S. J.; Berendsen, H. J. C. *Biochim. Biophys. Acta: Biomembr.* **1997**, *1331*, 235–270.
(15) Mueller, M.; Katsov, K.; Schick, M. *Phys. Rep.* **2006**, *434*, 113–176.
(16) Ginzburg, V. V.; Balijepalli, S. *Nano Lett.* **2007**, *7*, 3716–3722.
(17) Netz, R. R.; Schick, M. *Phys. Rev. E* **1996**, *53*, 3875–3885.
(18) Mornet, S.; Lambert, O.; Duguet, E.; Brisson, A. *Nano Lett.* **2005**, *5*, 281–285.
(19) Huang, S.-C. J.; Artyukhin, A. B.; Martinez, J. A.; Sirbuly, D. J.; Wang, Y.; Ju, J.-W.; Stroeve, P.; Noy, A. *Nano Lett.* **2007**, *7*, 3355–3359.
(20) Leroueil, P. R.; Hong, S. Y.; Mecke, A.; Baker, J. R.; Orr, B. G.; Holl, M. M. B. *Acc. Chem. Res.* **2007**, *40*, 335–342.
(21) Levene, M. J.; Korlach, J.; Turner, S. W.; Foquet, M.; Craighead, H. G.; Webb, W. W. *Science* **2003**, *299*, 682–686.
(22) Roiter, Y.; Minko, S. *J. Am. Chem. Soc.* **2005**, *127*, 15688–15689.
(23) Xie, A. F.; Yamada, R.; Gewirth, A. A.; Granick, S. *Phys. Rev. Lett.* **2002**, *89*, 246103/1–246103/4.
(24) Balgavy, P.; Dubnickova, M.; Kucerka, N.; Kiselev, M. A.; Yaradaikin, S. P.; Uhrikova, D. *Biochim. Biophys. Acta: Biomembr.* **2001**, *1512*, 40–52.
(25) Lipowsky, R.; Dobereiner, H. G. *Europhys. Lett.* **1998**, *43*, 219–225.
(26) Deserno, M.; Gelbart, W. M. *J. Phys. Chem. B* **2002**, *106*, 5543–5552.
(27) Fleck, C. C.; Netz, R. R. *Europhys. Lett.* **2004**, *67*, 314–320.
(28) Deserno, M. *J. Phys.: Condens. Matter* **2004**, *16*, S2061–S2070.
(29) Parthasarathy, R.; Groves, J. T. *Soft Matter* **2007**, *3*, 24–33.
(30) Nylund, M.; Fortelius, C.; Palonen, E. K.; Molotkovsky, J. G.; Mattjus, P. *Langmuir* **2007**, *23*, 11726–11733.

NL080080L